forests

MDPI

Article

Linking Tree Health, Rhizosphere Physicochemical Properties, and Microbiome in Acute Oak Decline

Diogo Pinho [1,2,*], Cristina Barroso [1,3], Hugo Froufe [1], Nathan Brown [4], Elena Vanguelova [4], Conceição Egas [1,3] and Sandra Denman [4,*]

1 Next Generation Sequencing Unit, UC-Biotech, Biocant Park, Núcleo 04 Lote 8, 3060-197 Cantanhede, Portugal; cristina.barroso@biocant.pt (C.B.); hugo.froufe@biocant.pt (H.F.); cegas@biocant.pt (C.E.)
2 Department of Biology and CESAM, University of Aveiro, Campus Santiago, 3810-193 Aveiro, Portugal
3 Center for Neuroscience and Cell Biology, University of Coimbra, Rua Larga Faculdade de Medicina, Pólo I, 1st floor, 3004-504 Coimbra, Portugal
4 Forest Research, Centre for Ecology, Biosecurity and Society, Farnham, Surrey GU10 4LH, UK; nathan@woodlandheritage.org (N.B.); elena.vanguelova@forestresearch.gov.uk (E.V.)
* Correspondence: diogo.pinho@biocant.pt (D.P.); sandra.denman@forestresearch.gov.uk (S.D.); Tel.: +44-(0)-300-067-5640 (S.D.)

Received: 27 September 2020; Accepted: 29 October 2020; Published: 30 October 2020

Abstract: Forest decline diseases are complex processes driven by biotic and abiotic factors. Although information about host–microbiome–environment interactions in agricultural systems is emerging rapidly, similar studies on tree health are still in their infancy. We used acute oak decline (AOD) as a model system to understand whether the rhizosphere physicochemical properties and microbiome are linked to tree health by studying these two factors in healthy and diseased trees located in three sites in different AOD stages—low, mid and severe. We found significant changes in the rhizosphere properties and microbiome composition across the different AOD sites and between the tree health conditions. Rhizosphere pH correlated with microbiome composition, with the microbial assemblages changing in more acidic soils. At the severe AOD site, the oak trees exhibited the lowest rhizosphere pH and distinct microbiome, regardless of their health condition, whereas, at the low and mid-stage AOD sites, only diseased trees showed lower pH and the microbial composition differed significantly from healthy trees. On these two sites, less extreme soil conditions and a high presence of host-beneficial microbiota were observed in the healthy oak trees. For the first time, this study gathers evidence of associations among tree health conditions, rhizosphere properties and microbiome as well as links aboveground tree decline symptoms to the belowground environment. This provides a baseline of rhizosphere community profiling of UK oak trees and paves the way for these associations to be investigated in other tree species suffering decline disease events.

Keywords: acute oak decline; decline disease; microbiome; rhizosphere; soil chemistry; tree health

1. Introduction

Forests are globally important systems [1], often damaged by disturbances, which leads to a significant loss of trees. This is of great concern as humans and environments rely on the functions, goods, and services provided by these essential ecosystems [1–3]. Among the far-reaching consequences of forest disturbance is tree decline and the onset of decline diseases. Decline diseases, defined by Manion and Lachance (1992) [4], are the result of the 'interaction of interchangeable, specifically ordered, abiotic and biotic factors that produce a general deterioration, often ending in the death of trees'. Three distinct phases in the decline process were recognised: predisposition,

inciting, and contributing [5]. Predisposition factors are those related, in general, to site resilience and involve long-term influences of the environmental and/or biological factors that weaken the host before the onset of decline. Inciting factors are short term and transient factors of biotic and/or abiotic origin, such as insect defoliating events, extreme weather conditions or human activities, amongst others. The contributing factors include secondary pests and diseases that can be very destructive to weakened trees and bring them to death. According to this concept, single or multiple factors within one category are not able, alone, to drive the decline [6]. Recent evidence suggests that tree decline disease interactions are more complex than previously envisaged, and occur at a range of scales spanning landscape to molecule [7,8]. In view of new research towards a deeper understanding of the mechanistic and functional components of plant–microbe interactions at the systems level [9], studies elucidating the drivers and mechanisms behind decline diseases in the UK are underway using oak decline as a platform for investigation.

There are only two native oak species in the UK, *Quercus robur* L. (pedunculate oak) and *Quercus petraea* (Matt.) Liebl. (sessile oak). Both are foundation species and susceptible to acute oak decline (AOD). This recent emerging threat is spreading through Britain's woodlands, parklands, urban landscapes, and gardens, raising much concern amongst landowners and managers as affected trees can rapidly decline over 3–5 years with a high number of symptomatic trees dying [10,11]. Bark cracks, necrotic inner tissues and dark exudates bleeding on the stems, and larval galleries of the buprestid beetle *Agrilus biguttatus* are the distinctive set of visible symptoms characterising the disease [10]. Similar symptoms have also been observed in continental European oaks [10]. The bacterial species *Rahnella victoriana*, *Brenneria goodwinii*, and *Gibbsiella quercinecans* have been consistently isolated from AOD lesions [12,13]. Using a contemporary approach for adapting and fulfilling Koch's postulates, *B. goodwinii* and *G. quercinecans* were proven capable of oak tissue necrosis, and together with the larvae of the beetle, formed the main symptoms of AOD [14]. Modern molecular ('omics') analyses of AOD symptomatic field material provided the link between *B. goodwinii* and *G. quercinecans* and lesion formation, where *B. goodwinii* has a dominant role [7]. Knowledge about the AOD pathobiome [7,14,15] and environmental factors that predispose oak trees to AOD [8] has led to remarkable advances in understanding and managing AOD in the UK. However, emerging evidence of 'the importance of the microbiome of the plant holobiont' (the holobiome) in host health emphasises the necessity for a better understanding of the microbiomes of the various niches of large, complex, long-living plants like trees [16,17]. A particularly important niche is the rhizosphere, as it is the link between nutrient and water supply and the host demand [16,18]. The rhizosphere has a specific chemistry, is rich in microbial diversity, abundance and activity [19], and is distinct from the bulk soil [20,21]. It is thought that bacterial and fungal communities in this environment have a pivotal role in contributing to tree health and fitness [16], while simultaneously and responsively, the host shapes its microbial assemblage [22]. Although some research on the rhizosphere microbiomes of several tree species has been reported [20,21,23–26], knowledge about the linkages among site factors, composition, and role of this specific niche microbiome concerning tree health condition is still lacking. Elucidating the relationships between microbial communities and forest hosts under decline disease disturbances is a complex process, which can be disentangled by gathering stepwise cumulative information. Moreover, to track the changes and differences in soil functions, functional properties are defined, which represent a way to assess soil health [27]. Soil carbon, nitrogen, phosphorus, pH, water content, and bulk density are the most commonly proposed indicators for soil function due to their impacts on a wide range of soil ecosystem services [28]. Soil acidity, carbon and nitrogen content, and the ratio of C:N are key determinants of various soil functions, including greenhouse gas emissions, biomass production, organic matter mineralization and decomposition, and influencing biological communities, but their exact impacts are often hard to evaluate [29].

As a starting point, this study describes and compares the physicochemical properties and microbiome of rhizosphere soils of healthy and AOD symptomatic pedunculate oak trees at three

UK sites to determine whether rhizosphere physicochemical properties and microbial communities changed according to the tree health condition.

2. Materials and Methods

2.1. Site Selection and Soil Sampling

Three parkland sites were selected based on the presence of pedunculate oak trees with AOD symptoms, the history of AOD monitoring and the willingness of landowners to allow access to the sites: Eastnor Castle Deer Park (Ledbury, UK, SO743371), low-stage AOD; Hatchlands Park (Guildford, UK, TQ067521), mid-stage AOD; and Richmond Park (London, UK, TQ202743), severe-stage AOD (Figure 1). The three sites represent a range of AOD developmental stages, which were defined based on AOD incidence and severity monitoring data (Figure 1). At Eastnor, AOD symptomatic trees were first reported in 2016 with a small proportion of trees lightly affected, whereas trees at Hatchlands have been monitored for AOD since 2009 with a moderate proportion of moderately affected trees. Although Richmond has only been intensively monitored since 2010 [30], this site has a long history of severe AOD presence with a high number of severely affected trees and high levels of tree mortality [31].

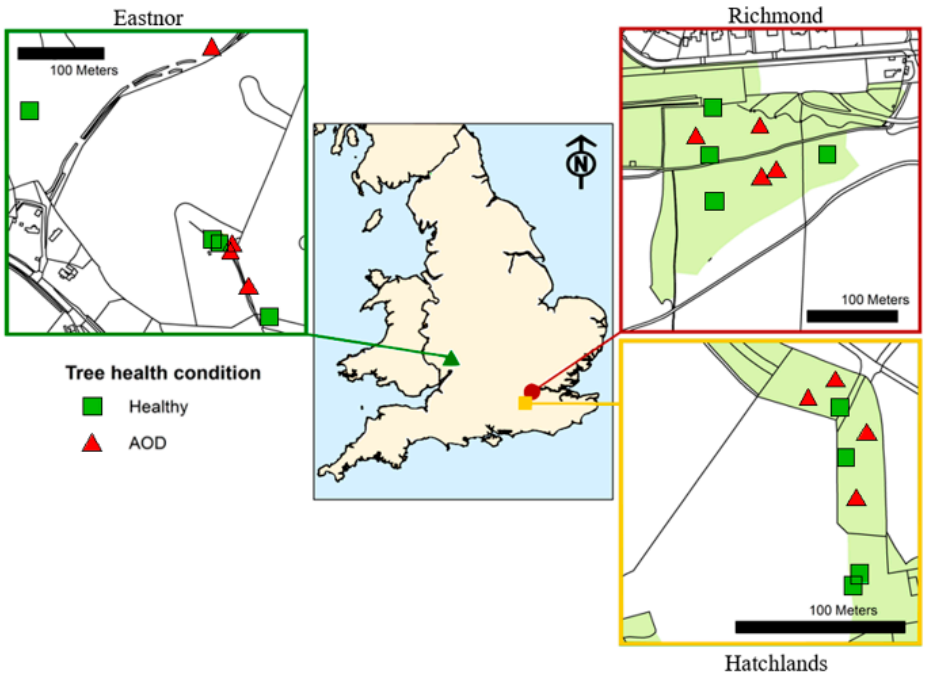

Site	Incidence (%)	Severity	Development Stage
Eastnor	Low (< 10)	Low (2.00)	Low
Hatchlands	Moderate (< 25)	Moderate (4.37)	Mid
Richmond	High (> 70)	High (7.02)	Severe

Figure 1. Location of the UK sites and sampled healthy (green square) and acute oak decline (AOD) (red triangle) trees in Eastnor (low-stage AOD, green), Hatchlands (mid-stage AOD, yellow), and Richmond (severe-stage AOD, red). Each point represents the specific GPS location of each sampled tree. The overview of the AOD developmental stage is presented in the table below the maps. AOD incidence and severity classifications were defined based on the monitoring data of the number of trees affected (percentage) and bleeds per tree (average number of bleeds per stem), respectively. AOD developmental stage was set by combining disease incidence and severity.

At each site, four healthy and four AOD trees were randomly selected (Figure 1) based on the Forest Research monitoring records, following the visual tree health condition criteria as previously reported [30]. The rhizosphere soils were collected after removing the top litter layer. At each tree, four cores were taken under the crown (2–4 m in approximate cardinal directions radially from the trunk), and the fine roots and attached rhizosphere soil were pooled in a single sterile bag. Samples were collected to a depth of 30 cm because the fine roots of trees are mainly distributed in this soil zone. Additionally, four single cores of bulk soil were randomly taken outside the vicinity of the tree root system (i.e., in surrounding open spaces within each site). The bulk soils were used as control samples to enable comparisons between soil the compartments and for the detection of oak rhizosphere effect. In total, 24 rhizosphere and 12 bulk soil samples were collected in November 2016 across Eastnor (low-stage AOD), Hatchlands (mid-stage AOD), and Richmond (severe-stage AOD), corresponding to 8 rhizosphere samples (4 healthy and 4 AOD trees) and 4 bulk soils per site.

2.2. Physicochemical Analysis

Rhizosphere soils were separated from the roots in the laboratory by gently shaking the roots and collecting the loosened soil. The rhizosphere and bulk soil samples were separately sieved through a 2 mm mesh, and *c.* 5 g of each soil sample was stored at −80 °C until DNA extraction. The remaining soil samples were analysed for moisture using the gravimetric method, pH (in water) using an automated Metrohm autosampler with a 719 S Titrino unit and a Sentek electrode, and total carbon (C) and total nitrogen (N) by dry combustion at 900 °C using a FlashEA1112 NC analyser (Thermo Fisher Scientific, Waltham, MA, USA). Soil C:N ratio was also calculated for each sample. The analyses were performed at the Chemical Analysis Laboratory of Forest Research, UK.

2.3. DNA Extraction, PCR Library Preparation, High-Throughput Sequencing and Data Processing

The DNA was extracted from 500 mg of each rhizosphere and bulk soil samples using the NucleoSpin Soil kit (Macherey-Nagel, Düren, Germany) with buffer SL2 and Enhancer SX according to the manufacturer's instructions. Soilless blank controls were included to ensure reagent sterility. Agarose gel electrophoresis, ND1000 spectrophotometer (NanoDrop Technologies, Wilmington, DC, USA) and Quant-iT PicoGreen dsDNA Assay Kit (Thermo Fisher Scientific, Waltham, MA, USA) were used to check the DNA quality and yield. The DNA samples were stored at −20 °C for further use.

The DNA extracted from the rhizosphere and bulk soil samples were used for the amplification and sequencing of the bacterial V3–V4 variable regions of the 16S rDNA, and the fungal Internal Transcribed Spacer 2 (ITS2). The bacterial primers used were: forward primer 341F 5′-CCTACGGGNGGCWGCAG-3′ and reverse primer 805R 5′-GACTACHVGGGTATCTAATCC-3′ [32,33]; and the fungal primers used were: forward primers pool ITS3NGS1_F 5′-CATCGATGAAGAACGCAG-3′, ITS3NGS2_F 5′-CAACGATGAAGAACGCAG-3′, ITS3NGS3_F 5′-CACCGATGAAGAACGCAG-3′, ITS3NGS4_F 5′-CATCGATGAAGAACGTAG-3′, ITS3NGS5_F 5′-CATCGATGAAGAACGTGG-3′, and ITS3NGS10_F 5′-CATCGATGAAGAACGCTG-3′, and reverse primer ITS3NGS001_R 5′-TCCTSCGCTTATTGATATGC-3′ [34].

The first PCR was performed using KAPA HiFi HotStart ReadyMix PCR Kit (Roche, Wilmington, MA, USA), 200 nM of each primer, and 12.5 ng of template environmental DNA in a total volume of 25 µL. The PCR conditions involved a 3 min denaturation at 95 °C, followed by 25 cycles of 98 °C for 20 s, 55 °C (V3-V4) or 60 °C (ITS2) for 30 s and 72 °C for 30 s and a final extension at 72 °C for 5 min in a Veriti 96-Well Thermal Cycler (Thermo Fisher Scientific, Waltham, MA, USA). Negative controls were included. PCR products were run on an agarose gel (1% w/v) and purified using Agencourt AMPure XP (Beckman Coulter, Brea, CA, USA) according to the manufacturer's instructions.

Dual indexes and Illumina sequencing adapters from the Nextera XT Index kit (Illumina, San Diego, CA, USA) were attached to both ends of the amplicons by limited-cycle PCR [35]. This second PCR used KAPA HiFi HotStart ReadyMix PCR Kit (Roche, Wilmington, MA, USA), 2.5 µL of each indexed adapter primer, and 2.5 µL of the first PCR product, in a total volume of 25 µL. PCR conditions

included 3 min denaturation at 95 °C, followed by 8 cycles at 95 °C for 30 s, 55 °C for 30 s and 72 °C for 30 s and a final extension at 72 °C for 5 min in a Veriti 96-Well Thermal Cycler (Thermo Fisher Scientific, Waltham, MA, USA). PCR products were checked on an agarose gel (1% w/v) and one-step purified and normalized using a SequalPrep Normalization Plate Kit (Thermo Fisher Scientific, Waltham, MA, USA). Amplicon libraries were pooled, and pair-end sequenced using the MiSeq Reagent Kit v3 in the MiSeq platform (Illumina, San Diego, CA, USA) at Genoinseq (Cantanhede, Portugal). All sequence data described in this study are available in the European Nucleotide Archive (ENA) under accession number PRJEB29902.

Sequence reads were quality-filtered using PRINSEQ version 0.20.4 [36]. Sequencing adapters and reads with less than 150 bp (bacteria) or 100 bp (fungi) were removed. Reads were trimmed where the average base quality was below Q25 in a window of 5 bp. The forward and reverse reads were merged by overlapping the paired-end reads with AdapterRemoval version 2.1.5 [37] using default parameters. Chimeric reads were removed using USEARCH version 6.1 [38]. The highly variable fungal ITS2 from the merged reads was extracted with ITSx version 1.0.11 [39]. The bacterial and fungal reads were clustered into operational taxonomic units (OTUs) at 97% of similarity using the open reference approach of the QIIME package version 1.8.0 [40]. Taxonomy was annotated using UCLUST [38] with the databases Greengenes version 13.8 [41] for bacteria or UNITE version 7.1 [42] for fungi. Singletons (OTUs represented by one single read) were removed from the OTU tables as well as OTUs annotated as Archaea, "Chloroplast" and "Mitochondria".

2.4. Total Abundance of Soil Bacterial and Fungal Communities

Total bacterial and fungal abundances were estimated by quantifying the copy number of the bacterial 16S rDNA and the fungal ITS2 using qPCR. Concentrated stock solutions (10^7 molecules μL^{-1}) of 16S and ITS amplicon standards were prepared by PCR amplification using the conditions described in the PCR library preparation. An equimolar pool of all soil samples was used as a template. For each DNA target, a set of calibration standards with known concentrations were generated by serial dilutions. Each sample and standard was quantified in triplicate using 2X Fast SYBR Green Master Mix (Thermo Fisher Scientific, Waltham, MA, USA), 0.5 µM of each PCR primer (the same used in library preparation) and 1 or 10 ng of template DNA for a bacteria or fungi assay in a total volume of 10 µL. The qPCR conditions involved a 20 s denaturation at 95 °C, followed by 40 cycles of 95 °C for 20 s, 58 °C for 15 s and 60 °C for 45 s for bacteria, and 20 s denaturation at 95 °C, followed by 40 cycles of 95 °C for 10 s, 60 °C for 45 s for fungi, in a 7500 Fast Real-Time PCR System (Thermo Fisher Scientific, Waltham, MA, USA). All qPCR assays included negative template controls using water instead of DNA.

2.5. Data Analysis

For alpha diversity analyses, the species richness was assessed using Chao1 (estimated number of OTUs) and the observed species (number of OTUs), and the species diversity was calculated using Pielou's Evenness, Shannon, and Simpson indexes. These parameters were calculated using the script alpha_diversity.py of the QIIME package version 1.8.0 [40].

The relationships across soil properties, microbiome composition, soil compartment, site, and tree health condition were investigated using PRIMER-E [43]. OTU tables were log (X + 1) transformed, and the Bray–Curtis similarity matrixes were calculated. Distance-based redundancy analysis (dbRDA) was then applied to explore the microbial and soil properties data according to soil compartment, site, and tree health condition. Permutational multivariate analysis of variance (PERMANOVA) was used to test the differences according to the stated factors. Correlations between microbiome composition and soil properties were tested using a non-parametric Mantel test (RELATE function of PRIMER-E) and the soil properties that best explained the bacterial and fungal community patterns were determined by BEST analysis [44] using the same software.

Fungi were sorted into ecologically meaningful categories by assigning ecological guilds to each community member, whenever possible, using FUNGuild [45].

Differential abundance analyses of each bacterial and fungal OTU detected in the rhizosphere soils across the sites and tree health conditions were performed using DESeq 2.0 [46] in the MicrobiomeAnalyst [47]. OTUs with less than two counts per sample and a prevalence of less than 20% across the samples were excluded. Moreover, OTUs with less than 10% variance, based on the interquartile range, were also removed. Variance stabilization transformation was applied using weighted trimmer mean of *M*-values (TMM). The analysis outputs were used to create Volcano plots using Microsoft Excel. Relative abundances of the significantly abundant fungi (FDR corrected $p < 0.05$) were visually represented in bar plots using Excel or in Circle Packing charts built using the open source framework RAW Graphs [48].

Analysis of variance (ANOVA) or the Kruskal–Wallis test were performed, where applicable, to assess the differences according to soil compartment, site, and tree health condition. Pairwise comparisons were assessed using Tukey's HSD post hoc or Mann–Whitney U test. All assumptions were checked before statistical analysis. IBM SPSS statistics 22 [49] was used to carry out the statistical analysis.

3. Results

3.1. Physicochemical Properties and Microbiome Are Different in the Rhizosphere and Bulk Soil Compartments

The physicochemical properties and microbiome composition differed between the oak rhizosphere and bulk soil compartments in all three sites (Tables S1 and S2, Figure S1). At Richmond, the rhizosphere soil was significantly more acidic (pH 4.33 ± 0.14) compared to the bulk soil (5.12 ± 0.07; $p < 0.001$; Table S1). Bulk soil and rhizosphere pH were similar at Eastnor and Hatchlands (average of 5.66 and 5.92, respectively). The total C, N, and the C:N ratio were significantly higher in the rhizosphere than in the bulk soil compartment across all the sites ($p < 0.001$). In particular, the rhizosphere at Richmond showed eight times more C (225,966 ± 55,586 mg/soil kg) and six times more N (12,921 ± 3,331 mg/soil kg) compared to the bulk soil (Table S1). In general, microbial diversity in rhizosphere soil was slightly higher compared to the bulk soil (Table S2). The soil compartments differed significantly in their microbiome composition, for both bacteria (Pseudo-F = 4.61, $p < 0.01$) and fungi (Pseudo-F = 8.04, $p < 1 \times 10^{-5}$) across the three sites (Figure S1). The results show that the soil properties and microbial communities are specific to the soil compartment. To further characterize the rhizosphere properties and microbiome and their relation with site and tree health conditions, we excluded the bulk soil data because it is likely that this niche has different drivers from those found in the rhizosphere.

3.2. Rhizosphere Physicochemical Properties Differ across Sites and Tree Health Conditions

The rhizosphere physicochemical properties varied significantly among the sites, in which Richmond showed the largest differences, and Eastnor and Hatchlands had identical rhizosphere properties (Table 1). The rhizosphere soil at Richmond was significantly more acidic (mean = 4.33; $p < 0.001$), the total C concentration was 3.6 times higher (225,966 mg/soil kg on average; $p < 0.01$) and the N concentration 2.8 times higher (12,922 mg/soil kg, $p < 0.01$), than the other two sites (62,478 and 4,605 mg/soil kg, respectively). (Table 1). Besides, the C:N ratio increased significantly ($p < 0.01$) across the sites, in which Eastnor had the lowest values and Richmond the highest (Table 1).

When comparing the healthy and diseased trees within each site, there were significant differences ($p < 0.05$) in the rhizosphere soil pH (Table 1). At Hatchlands, the rhizosphere soil of AOD symptomatic trees was significantly ($p < 0.001$) more acidic (pH ranging from 4.84 to 5.74) compared to healthy trees (pH 5.59–7.52) and a very similar tendency was observed at Eastnor. However, no differences were detected at Richmond, where in both healthy and diseased trees, rhizosphere soils were very acidic (pH 4.14–4.49) (Table 1).

Table 1. Physicochemical properties of the oak rhizosphere soils across the sites and tree health conditions.

Site	AOD Stage	Tree Health Condition	Moisture (%) *	pH (H_2O) ***	Total C (mg/kg) **	Total N (mg/kg) **	C:N Ratio **
Eastnor	Low	Healthy	30 ± 1 ^{a}	6.09 ± 0.22 ^{ab}	61,810 ± 4,991 ^{a}	4,877 ± 439 ^{a}	12.69 ± 0.38 ^{a}
		AOD	19 ± 1 ^{c}	5.27 ± 0.31 ^{b}	59,670 ± 15,330 ^{a}	4,380 ± 729 ^{a}	13.40 ± 1.36 ^{ab}
Hatchlands	Mid	Healthy	24 ± 3 ^{bc}	6.43 ± 0.70 ^{a}	64,834 ± 13,077 ^{a}	4,739 ± 989 ^{a}	13.70 ± 0.56 ^{b}
		AOD	20 ± 1 ^{c}	5.42 ± 0.24 ^{b}	63,598 ± 3,852 ^{a}	4,423 ± 480 ^{a}	14.46 ± 0.83 ^{b}
Richmond	Severe	Healthy	27 ± 7 ^{ab}	4.35 ± 0.13 ^{c}	228,313 ± 53,690 ^{b}	12,905 ± 3,356 ^{b}	17.83 ± 0.58 ^{c}
		AOD	26 ± 6 ^{abc}	4.30 ± 0.14 ^{c}	223,618 ± 57,324 ^{b}	12,938 ± 3,305 ^{b}	17.28 ± 0.36 ^{c}

Mean values of soil physicochemical parameters ± standard deviation are shown (n = 24). Asterisks and letters indicate significant differences as determined by statistical analysis (* for $p < 0.05$; ** for $p < 0.01$; *** for $p < 0.001$).

3.3. Taxonomic Distribution of Oak Rhizosphere Microbiome

Single gene community profiling took place on high-quality isolated DNA. Yields of 1,661,144 and 1,647,971 16S rDNA and ITS2 high-quality reads were obtained, clustering into 36,841 and 6519 bacterial and fungal OTUs at 97% distance sequence similarity, respectively (Tables S3 and S4).

Regardless of the site and tree health condition, Proteobacteria (28.1%), Actinobacteria (24.8%), Acidobacteria (17.4%), Verrucomicrobia (9.5%), Planctomycetes (7.8%), Firmicutes (3.2%), Bacteroidetes (2.8%), and Choroflexi (2.0%) were the eight dominant phyla, totalling 95.5% of the entire bacterial community (Figure 2a). In the fungal community, 82.8% of the identified OTUs were assigned to Basidiomycota (41.5%), Ascomycota (32.1%), and Zygomycota (15.1%; currently circumscribed as Mucoromycota and Zoopagomycota [50]) phyla and the unidentified fungi represented 10.3% of the total fungal community (Figure 2b). The remaining 37 bacterial and five fungal detected phyla, which individually represented less than 1% of the total community, were grouped in a group called "Other" and only accounted for 4.5% and 1.0% of all bacterial and fungal taxa, respectively (Figure 2).

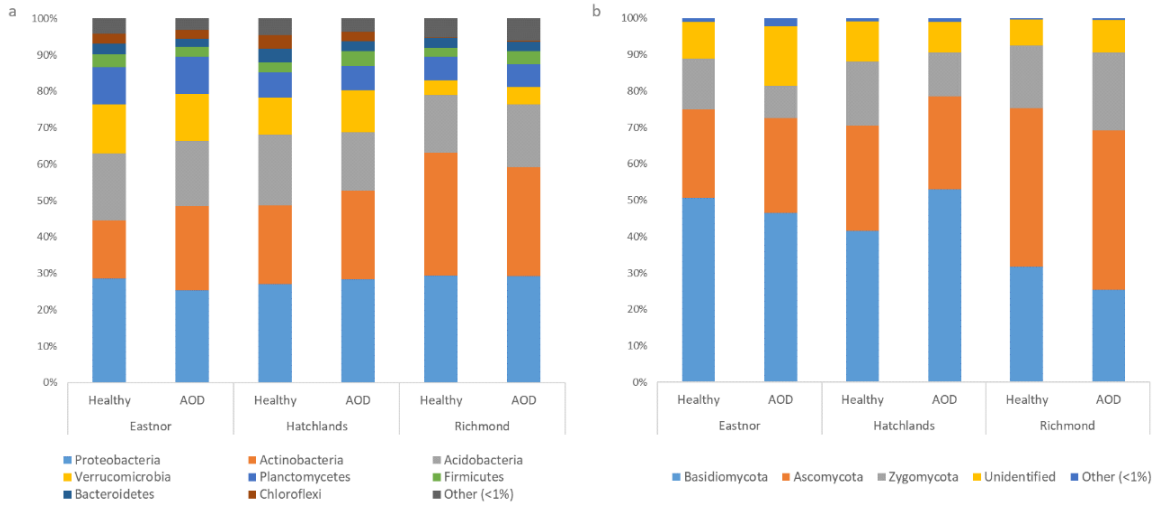

Figure 2. Relative abundance of the bacterial (**a**) and fungal (**b**) phyla detected in the rhizosphere of the healthy and AOD trees in Eastnor Park, Hatchlands Park, and Richmond Park (n = 24). The phyla that individually represented less than 1% of the total community were grouped in the artificial group "Others". For bacteria: Gemmatimonadetes, Nitrospirae, WPS-2, WS3, TM7, unidentified bacteria, Elusimicrobia, Chlamydiae, AD3, Armatimonadetes, Cyanobacteria, TM6, OD1, BRC1, Chlorobi, Tenericutes, Fibrobacteres, FBP, OP3, FCPU426, OP11, WS2, WS4, Spirochaetes, WS6, BHI80-139, GN02, NKB19, GAL15, NC10, [Thermi], Lentisphaerae, MVP-21, Aquificae, GN04, Kazan-3B-28, and WS5. For fungi: Rozellomycota, Chytridiomycota, Glomeromycota, Blastocladiomycota, and Microsporidia.

3.4. Oak Rhizosphere Microbiome Composition Differs across Sites and Tree Health Conditions

We sampled the rhizosphere soils of 12 healthy and 12 AOD oak trees across three sites with different AOD developmental stages: Eastnor (low-stage AOD), Hatchlands (mid-stage AOD) and Richmond (severe-stage AOD).

Bacterial diversity was more impacted than fungal diversity according to site (Table S5). Richmond showed significantly lower bacterial diversity compared to Eastnor and Hatchlands ($p < 0.05$), which had similar diversity to each other. The total abundance of bacteria was similar across all three sites. The bacterial diversity was similar between the healthy and AOD oaks within each site, and their total abundance varied significantly with no specific trend between the two health conditions (Table S5; $p < 0.05$). The fungal diversity and total abundance were similar across the sites and tree health conditions (Table S5).

However, the rhizosphere microbiome composition varied significantly across the sites and tree health conditions, as indicated by dbRDA and PERMANOVA (Figure 3 and Table S6;

$p < 0.05$). Richmond rhizospheres clustered separately from those of Eastnor and Hatchlands (Figure 3). PERMANOVA confirmed that the bacterial (Pseudo-F = 10.53, $p < 1 \times 10^{-5}$) and fungal (Pseudo-F = 6.43, $p < 1 \times 10^{-5}$) compositions changed significantly across the sites (Table S6; $p < 0.05$). Pairwise comparisons revealed that Richmond differed significantly from Eastnor and Hatchlands, where bacterial community composition was similar (Table S6; $p < 0.05$). The fungal composition varied significantly across all the sites (Table S6; $p < 0.05$).

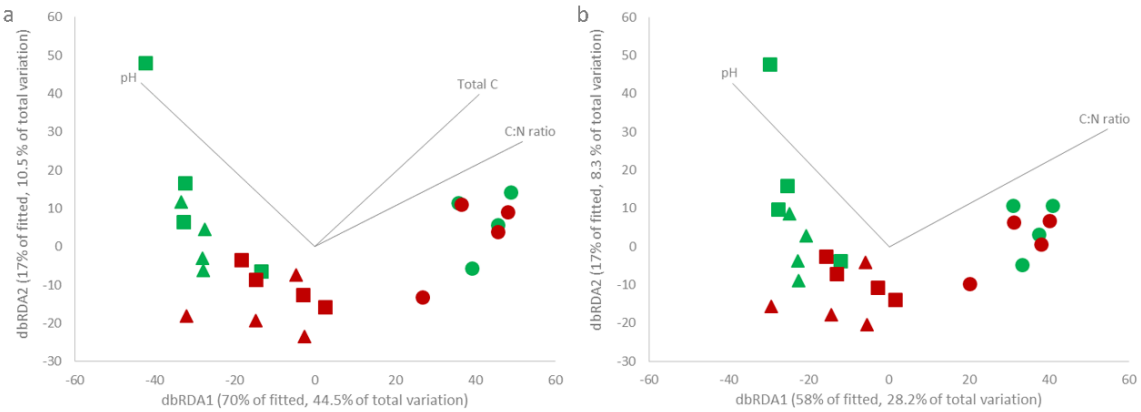

Figure 3. Distance-based redundancy analysis of the bacterial (**a**) and fungal (**b**) communities and rhizosphere soil chemical properties of the healthy and AOD trees across the sites ($n = 24$). The soil parameters determined by BEST analysis are shown in each plot. The longer the line, the stronger the correlation between the microbiome composition and the soil chemistry. Eastnor—triangle; Hatchlands—square; Richmond—circle; healthy trees—green; AOD trees—red.

Within Eastnor and Hatchlands, healthy and AOD trees clustered into two distinct groups. The dbRDA and PERMANOVA results showed that the microbiome composition in the healthy oak trees was significantly different from the AOD trees for both the bacterial (Pseudo-F = 3.37, $p < 0.05$) and fungal (Pseudo-F = 1.90, $p < 0.05$) communities (Figure 3, Table S6). No differences were observed in Richmond.

3.5. Rhizosphere Microbiome and Physicochemical Properties Are Correlated

The rhizosphere physicochemical properties and microbiomes showed strong correlation for both bacterial (Mantel r = 0.81, $p < 0.001$) and fungal (Mantel r = 0.73, $p < 0.001$) communities. Among the rhizosphere properties evaluated in this study, the BEST analysis revealed that rhizosphere pH was constantly present in all the combinations that best explained microbiome composition variance (Table S7), together with total C, and C:N for bacteria (Spearman's rs = 0.896, $p < 0.01$; Table S7) and C:N ratio for fungi (Spearman's rs = 0.848, $p < 0.01$; Table S7).

3.6. Rhizosphere Bacteria and Fungi Members Differ across the Sites and Tree Health Conditions

According to the differential abundance analysis (DESeq 2.0), Eastnor and Hatchlands shared many common rhizosphere members (Figure 4a,d), only differing in 13 bacterial and 101 fungal OTUs ($p < 0.05$). However, a considerable number of rhizosphere bacterial and fungal members differed from Richmond: 2237 bacterial and 409 fungal OTUs differed significantly ($p < 0.05$) between Eastnor and Richmond (Figure 4b,e), and 2,842 bacterial and 430 fungal OTUs between the Hatchlands and Richmond (Figure 4c,f; $p < 0.05$).

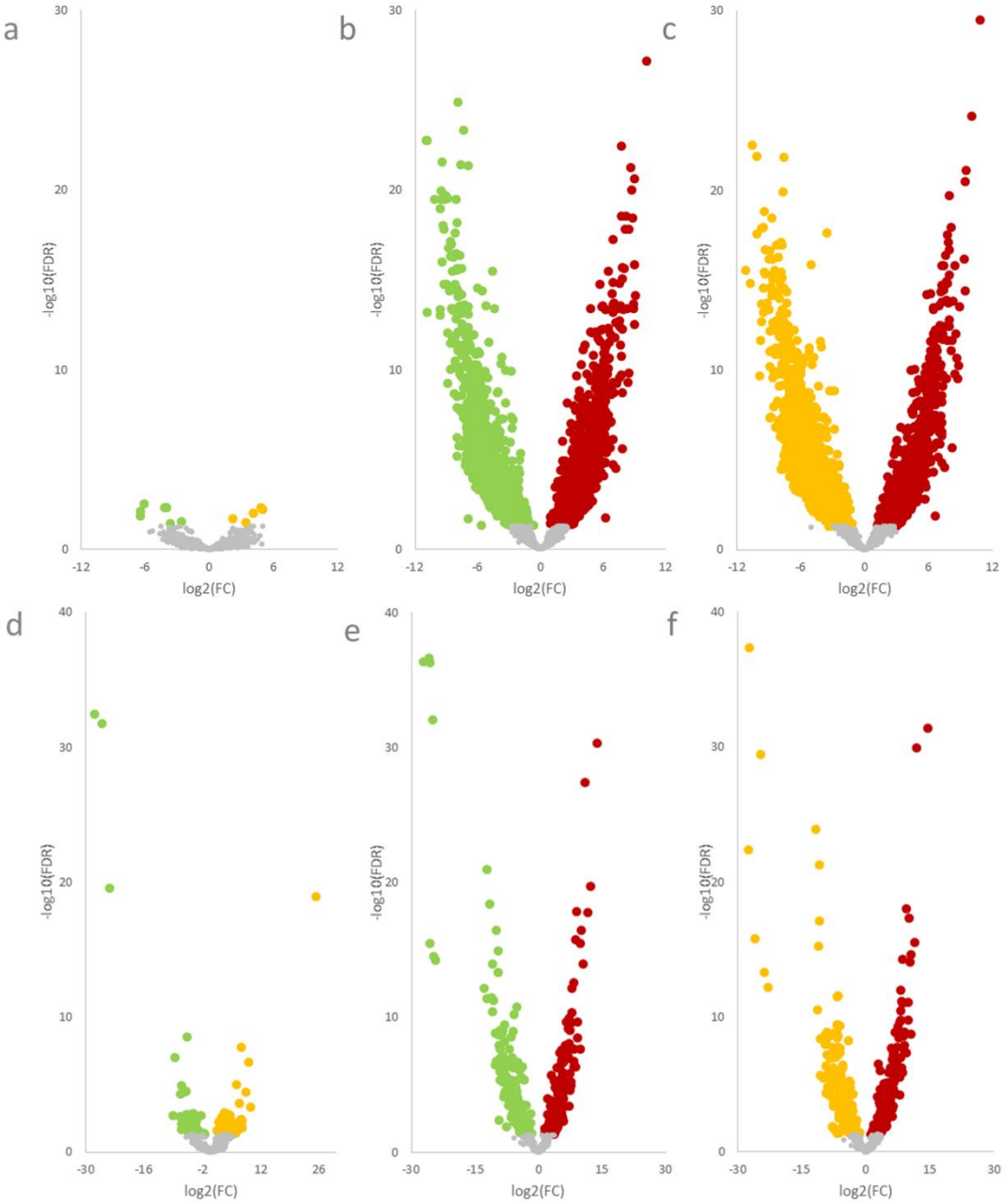

Figure 4. Volcano plots of differential bacterial (**a**–**c**) and fungal (**d**–**f**) operational taxonomic unit (OTU) abundance analysis as calculated by DESeq 2.0 according to the site (**a** and **d**—Eastnor vs. Hatchlands; **b** and **e**—Eastnor vs. Richmond; **c** and **f**—Hatchlands vs. Richmond). Fold change FDR corrected *p*-values are plotted for each OTU. Significantly different taxa (FDR-corrected $p < 0.05$) are coloured according to site: Eastnor—green, Hatchlands—yellow, Richmond—red.

When looking at the top 20 bacterial OTUs showing the highest fold change (negative fold change in Eastnor or Hatchlands and positive fold change in Richmond, Figure 5), members from the phyla Verrucomicrobia and Actinobacteria were particularly enriched at Eastnor and Hatchlands sites. Richmond showed a higher abundance of the families *Acidobacteriaceae* (phylum Acidobacteria), *Acetobacteraceae*, *Rhodospirillaceae* (class Alphaproteobacteria), *Sinobacteraceae*, and *Xanthomonadaceae* (class Gammaproteobacteria).

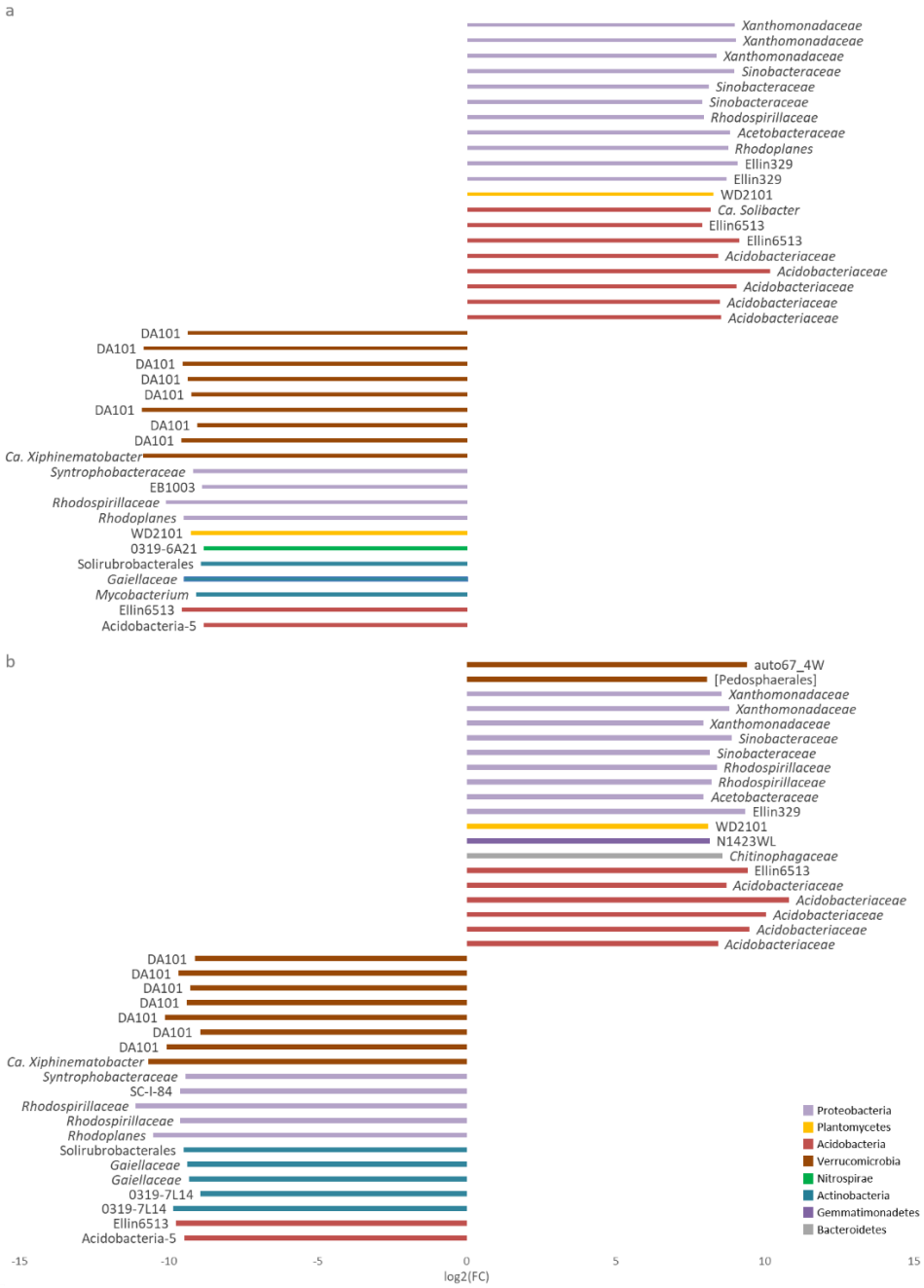

Figure 5. Differentially abundant OTUs between Eastnor–Richmond (**a**) and Hathclands–Richmond (**b**). The top 20 (the highest log2 fold changes) significantly enriched OTUs determined by DESeq 2.0 are depicted (FDR-corrected $p < 0.05$). Negative log2 (FC): Eastnor (**a**) and Hatchlands (**b**); Positive log2 (FC): Richmond (**a** and **b**).

Moreover, the members of the subdivision 6 Acidobacteria, Chloracidobacteria, and the phylum Nitrospirae were more abundant in Eastnor and Hatchlands (Table S8). On the other hand, the families *Burkholderiaceae* (class Betaproteobacteria) and *Sphingobacteriaceae* (phylum Bacteroidetes) were particularly enriched in Richmond (Table S8).

In the fungal community, DESeq 2.0 (Figure 6a) and FUNGuild (Figure 6b,c) analyses showed concordant results. The relative abundance of ectomycorrhizal fungal (EcM) was significantly higher ($p < 0.05$) at Eastnor (38 ± 11%) and Hatchlands (47 ± 12%) compared to Richmond (10 ± 3%; Figure 6b), namely *Cortinarius*, *Hebeloma*, *Humaria*, *Gymnomyces*, *Tomentella*, *Xerocomellus* and *Tuber* (Figure 6a and Figure S2). *Russula* and *Cenococcum* were particularly enriched at Richmond (Figure 6a and Figure S2).

In contrast, the percentage of saprobes in the rhizosphere was significantly lower ($p < 0.05$) in Eastnor (39 ± 10%) and Hatchlands (33 ± 9%) than in Richmond (64 ± 6%; Figure 6c), where *Aspergillus*, *Penicillium*, *Byssonectria*, *Nadsonia*, representatives of the phylum Zygomycota (currently circumscribed as Mucoromycota and Zoopagomycota [50]), and some plant pathogens, such as *Phaeoacremonium* and *Gibberella*, were particularly enriched (Figure 6a and Figure S2).

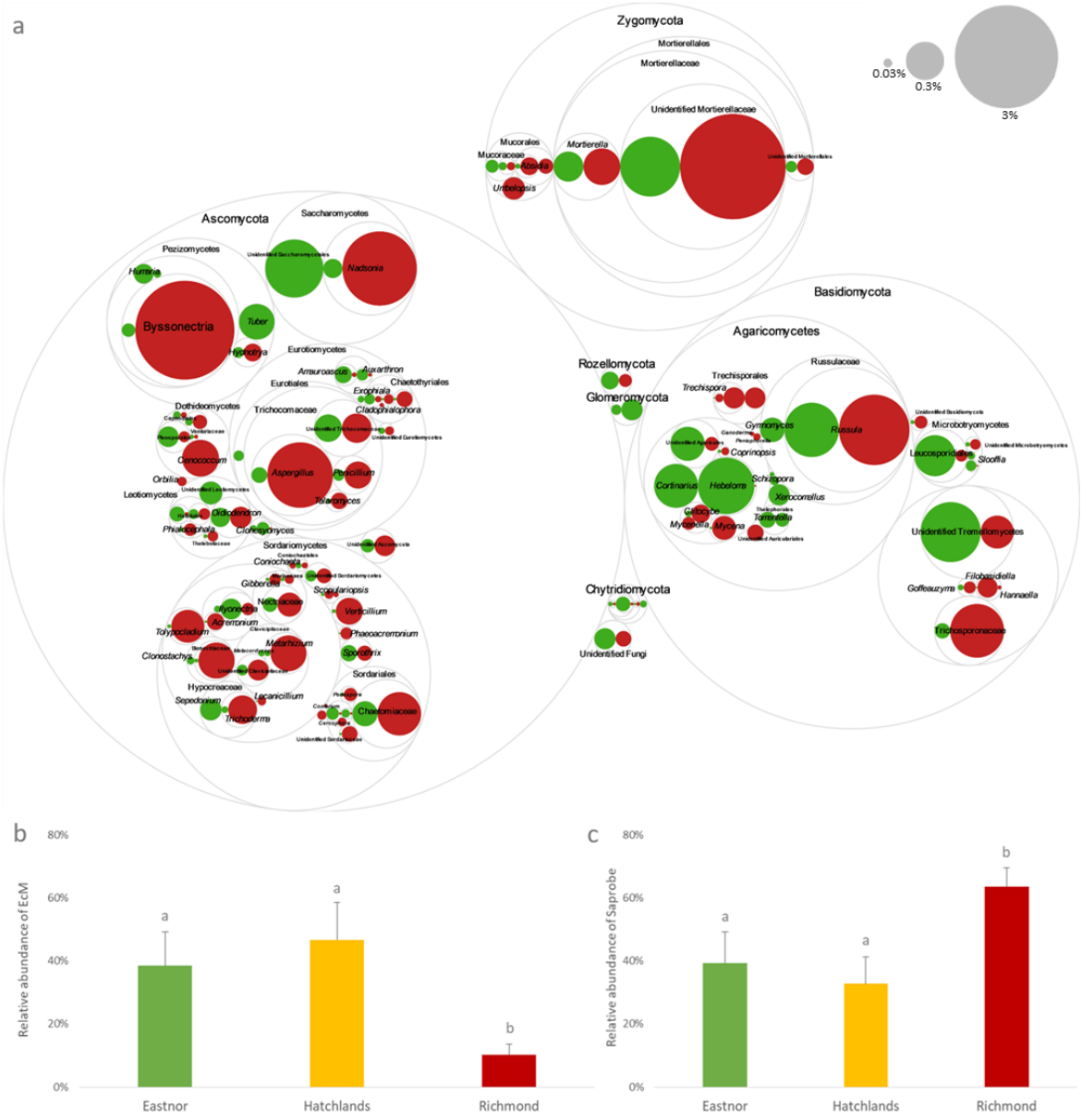

Figure 6. Fungi differentially abundant across the sites (**a**). Only significantly enriched OTUs determined by DESEq 2.0 are depicted (FDR-corrected $p < 0.05$). The size of the circles represents the relative abundance (scale represented by gray circles) and the colour denotes the rhizosphere of oak trees located in Eastnor (green) or Richmond (red) only. Ecological guilds of fungal taxa detected in the rhizosphere soils in Eastnor, Hatchlands, and Richmond (**b** and **c**). Significant differences ($p < 0.05$) according to the site are indicated by different letters. EcM—ectomycorrhizal fungi (**b**); saprobe—saprophytic fungi (**c**).

As revealed above by dbRDA and PERMANOVA, healthy trees held different microbial compositions compared to AOD trees at Eastnor and Hatchlands. Accordingly, the differential abundance analysis (DESeq 2.0) detected 848 bacterial and 70 fungal OTUs more abundant in healthy

trees, and 436 bacterial and 58 fungal OTUs enriched in AOD trees (Figure S3). No significant bacterial OTUs were detected between the healthy and AOD trees at Richmond (Figure S3).

Remarkably, similar taxa found in Eastnor (low-AOD stage) and Hatchlands (mid-AOD stage) were also enriched in the healthy trees. Among them, stood out the Chloracidobacteria (RB41), subdivision 6 Acidobacteria (iii1-15, mb2424, and RB40; phylum Acidobacteria), Nitrospira, and 0319-6A21 (phylum Nitrospirae), which were consistently more abundant (Figure 7). In the fungal community, few common OTUs were detected across the tree health comparisons but instead, they were site-specific (Figure S4).

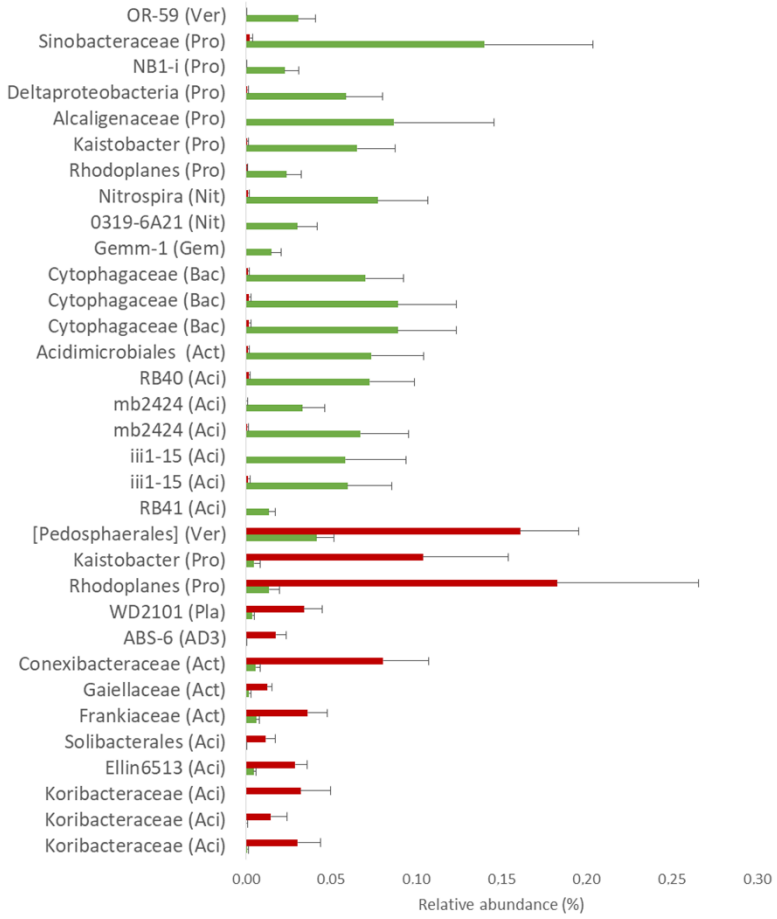

Figure 7. Relative abundance of the common bacterial OTUs, differentially abundant between healthy and AOD oaks across the tree health comparisons. Phyla are indicated in brackets: Ver—Verrucomicrobia; Pro—Proteobacteria; Nit—Nitrospirae; Gem—Gemmatimonadetes; Bac—Bacteroidetes; Act—Actinobacteria; Aci—Acidobacteria; Pla—Planctomycetes. Error bars are shown as SEM. Green bar—healthy oaks; red bar—AOD oaks.

4. Discussion

In this work, we studied the rhizosphere physicochemical properties and microbiome (bacteria and fungi) of healthy and AOD symptomatic trees across three UK sites that ranged from different stages of the disease. We showed that the host health, the rhizosphere physicochemical properties, and microbiome are linked at both site and tree conditions.

Across the three study sites (Figure 1), Richmond suffered the longest and the most severe AOD symptoms (severe-AOD stage) but also had the most unfavourable soil environment. The soil was very acidic, dry, compacted and generally low in C and N content. Trees respond and adapt to unfavourable soil environments and this can take place through various mechanisms, including changes in root exudation and rhizodeposition, which consequently change the rhizosphere soil properties [51–53]. In particular, plants can acidify their rhizosphere to facilitate nutrient uptake [54].

It is likely that all the oaks in Richmond have acidified their rhizosphere, regardless of tree health condition, in an effort to counter the poor soil environment and mobilize more nutrients for uptake to sustain growth and defence. At this site (severe-AOD stage), which showed the lowest rhizosphere pH, acidification dramatically boosted C and N levels in the rhizosphere compared to bulk soil, and these elements were higher than those measured at Eastnor and Hatchlands (low and mid-stage AOD sites, respectively). The same rhizosphere acidification trend/effect occurred in the AOD affected trees at Eastnor and Hatchlands. Rhizosphere acidification seems to be an important oak response to withstand unfavourable environmental conditions and disease establishment, raising the hypothesis that oaks may trigger pH-related mechanisms to cause an increase in acidity levels when affected by or indeed leading to AOD. The understanding of oak stress reaction mechanisms is still lacking, and experimental work is required to detail and prove the mechanisms used by trees in responding and adapting to abiotic and biotic stress factors.

Rhizosphere acidification can also affect microbiome composition. Firstly, we found that the rhizosphere and bulk soil compartments differed in their microbial assemblies. This rhizosphere effect, triggered by root exudates and rhizodeposition, has been reported in many tree species, including oak [21], beech, spruce [20], poplar [24,55], wherein a diverse array of root exudates selecting inhabiting microorganisms [56] with pivotal roles for host health, growth promotion, and productivity [16,19]. Proteobacteria, actinobacteria and Acidobacteria as well as Basidiomycota, Ascomycota, and Zygomycota (currently circumscribed as Mucoromycota and Zoopagomycota [50]) were the main colonizers of the oak rhizosphere, as previously reported on *Quercus* species and other woody plants [20,21,24,55].

In the second instance, here, we show that the rhizosphere microbiome changed according to health conditions at both site and tree conditions. Oaks at Richmond (severe-AOD stage) showed the most dissimilar rhizosphere microbiome, whereas the oak trees at Eastnor and Hatchlands (low- and mid-stage AOD) presented a microbial composition dependent on the host health condition. Indeed, root exudates can change in quantity and quality in response to external stressors and affect the rhizosphere microbial community [57,58]. The rhizosphere pH strongly and consistently correlated with rhizosphere microbiome composition, with the bacterial and fungal assemblages changing in more acidic soils. It is well established that soil pH is one of the most important drivers in structuring soil bacterial and fungal communities and it has been reported as a predictor of the diversity and composition of soil communities ([59], and references within).

Acidobacteria of the subdivision 6 and Chloracidobacteria, and members of the phylum Nitrospirae were consistently more abundant in healthy trees at Eastnor and Hatchlands, the low- and mid-stage AOD sites. Representatives of the phylum Acidobacteria are active members in the rhizosphere [60], capable of degrading complex plant polysaccharides [61], and harbouring putative extracellular peptidase genes for ammonium mobilization in N cycling [62]. Moreover, they have recently been suggested as potential plant growth promoters [63]. The phylum Nitrospirae includes essential members for nitrogen cycling [64]. Whether the beneficial role of subdivision 6 Acidobacteria, Chloracidobacteria, and Nitrospirae on tree health remains speculative, it deserves further research to understand their increased abundance in healthier conditions and association with AOD.

In our study, ectomycorrhizal (EcM) fungi, which establish essential mutualistic relations with oak trees [65,66], also varied in abundance and composition. At Eastnor and Hatchlands, EcM were more abundant and characterized by N-sensitive EcM fungi (e.g., *Cortinarius* and *Hebeloma*), whereas, at Richmond, this community was diminished and its profile enriched in nitrophilic and acidophilous EcM fungi (e.g., *Russula*). Suz et al. (2014) [67] reported similar shifts of EcM abundance and composition across European temperate oak forests. These shifts were explained by the differences detected in rhizosphere soil pH and N content across the sites and were reported as drivers of changes in these communities [67,68]. Other studies at local and continental scales also reported a reduction of EcM and changes in community profile with increasing N and decreasing pH [67–72]. However, our study

is the first report of this occurrence linked to pH on oak in the UK and specifically associated with AOD symptomatic trees.

Interestingly, we found bacteria and fungi previously linked to plant diseases and that were more abundant in oak rhizospheres at Richmond (severe-AOD stage). Examples include members of the families *Burkholderiaceae* and *Xanthomonadaceae*, which were also isolated from tissues of oaks affected with AOD [13]; representatives of the families *Sphingobacteriaceae* and *Burkholderiaceae*, which were reported in plant rhizospheres after pathogen infection [73]; and plant pathogenic fungi such as *Gibberella* [74,75] and *Phaeoacremonium* [76]. Moreover, saprophytic fungi were also more abundant at Richmond as well as in the AOD trees. This suggests that declining trees have poor feeder root health and are undergoing partial root degradation or are too weak to fend off saprophytic attack. Thus, such organisms are able to take advantage of the situation, which is evidenced by the enrichment in bacteria and fungi with a saprophytic lifestyle and is a consequence of probable high decay material availability. Indeed, the results are supported by previous studies also reporting soil microbiome changes caused by biotic and abiotic forest disturbances, particularly the increase in saprophytic taxa over beneficial species [77,78].

5. Conclusions

At first sight, our results appear to be a consequence of system perturbation that occurs in AOD establishment, in which the root exudation chemistry altered the rhizosphere soil pH and consequently changed the associated microbiome. However, the flip side of the results presented here raise the exciting hypothesis that the underground rhizosphere communities can potentially protect oaks against the AOD, a decline disease with aboveground symptoms. Understanding how trees and their associated microbiome respond to forest decline disease episodes is vital for providing in-depth knowledge to develop more efficient, affordable, sustainable, and reliable forest management strategies for the proactive prediction and mitigation of these events. In this sense, the present study gathers evidence of associations among tree health conditions, rhizosphere microbiome, and soil environment and paves the way for these associations to be investigated in other tree species suffering decline disease events.

Supplementary Materials: The following are available online at http://www.mdpi.com/1999-4907/11/11/1153/s1, Figure S1: Distance-based redundancy analysis of the (a) bacterial and (b) fungal communities and soil properties of the rhizosphere and bulk soil across the sites (n = 36), Figure S2: Fungi differentially abundant across the sites, Figure S3: Volcano plots of differential bacterial (a, b, c, d, and e) and fungal (f, g, h, I and j) OTU abundance analysis as calculated by DESeq 2.0 according to tree health condition, Figure S4: Venn diagram of the intersection of the differentially abundant fungal OTUs between healthy and AOD trees detected across the tree health comparisons, Table S1: Physicochemical properties according to soil compartment, Table S2: Microbial alpha diversity and total abundance according to soil compartment across the sites, Table S3: Bacterial OTU table, Table S4: Fungal OTU table, Table S5: Microbial alpha diversity and total abundance of the oak rhizosphere soils across the sites and tree health conditions, Table S6: PERMANOVA and pairwise comparison results of the comparison of the bacterial and fungal community according to the site and tree health condition (n = 24), Table S7: Combinations of rhizosphere soil explanatory variables that best explain the variance in the rhizosphere microbiome (n = 24), Table S8: Differentially abundant OTUs between Eastnor-Hatchlands, Eastnor-Richmond, and Hathclands-Richmond.

Author Contributions: Conceptualization, D.P., C.E., E.V. and S.D.; methodology, D.P., C.B., H.F., N.B., E.V., C.E., and S.D.; formal analysis, D.P., C.B. and H.F.; writing—original draft preparation, D.P.; writing—review and editing, D.P., E.V., C.E. and S.D.; supervision, C.E. and S.D.; project administration, S.D.; funding acquisition, S.D. All authors have read and agreed to the published version of the manuscript.

Funding: This research was funded by Defra as part of the Future Proofing Plant Health project and the Forestry Commission, and partly supported by the Strategic Project of Center for Neuroscience and Cell Biology (POCI-01-0145-FEDER-007440, strategic project UID/NEU/04539/2019). D.P. was supported by a Ph.D. grant from Fundação para a Ciência e a Tecnologia (SFRH/BD/100665/2014) and COST Action FP1305 grant (ECOST-STSM-FP1305-071116-080698). H.F. was supported by the GenomePT project (POCI-01-0145-FEDER-022184).

Acknowledgments: The authors would like to thank Aneta Dębicka for their assistance in the fieldwork and Kelly Scarlett for valuable, helpful discussion. We also thank the landowners for site access and allowing soil sampling.

Conflicts of Interest: The authors declare no conflict of interest. The funders had no role in the design of the study; in the collection, analyses, or interpretation of data; in the writing of the manuscript, or in the decision to publish the results.

References

1. Trumbore, S.; Brando, P.; Hartmann, H. Forest health and global change. *Science* **2015**, *349*, 814–818. [CrossRef] [PubMed]
2. Boyd, I.; Freer-Smith, P.; Gilligan, C.; Godfray, H. The consequence of tree pests and diseases for ecosystem services. *Science* **2013**, *342*, 1235773. [CrossRef] [PubMed]
3. Pautasso, M.; Schlegel, M.; Holdenrieder, O. Forest Health in a Changing World. *Microb. Ecol.* **2015**, *69*, 826–842. [CrossRef] [PubMed]
4. Manion, P.D.; Lachance, D. Forest decline concepts: An overview. In *Forest Decline Concepts*; Manion, P.D., Lachance, D., Eds.; APS Press: St. Paul, MN, USA, 1992; pp. 181–190.
5. Manion, P.D. *Tree Disease Concepts*, 2nd ed.; Manion, P.D., Ed.; Prentice-Hall, Inc.: Englewood Cliffs, NJ, USA, 1981.
6. Ciesla, W.M.; Donaubauer, E. *Decline and Dieback of Trees and Forests: A Global Overview*; Food and Agriculture Organization of the United Nations: Rome, Italy, 1994; ISBN 9251035024.
7. Broberg, M.; Doonan, J.; Mundt, F.; Denman, S.; McDonald, J.E. Integrated multi-omic analysis of host-microbiota interactions in acute oak decline. *Microbiome* **2018**, *6*, 21. [CrossRef] [PubMed]
8. Brown, N.; Vanguelova, E.; Parnell, S.; Broadmeadow, S.; Denman, S. Predisposition of forests to biotic disturbance: Predicting the distribution of Acute Oak Decline using environmental factors. *For. Ecol. Manag.* **2018**, *407*, 145–154. [CrossRef]
9. Levy, A.; Conway, J.M.; Dangl, J.L.; Woyke, T. Elucidating Bacterial Gene Functions in the Plant Microbiome. *Cell Host Microbe* **2018**, *24*, 475–485. [CrossRef] [PubMed]
10. Denman, S.; Brown, N.; Kirk, S.; Jeger, M.; Webber, J. A description of the symptoms of Acute Oak Decline in Britain and a comparative review on causes of similar disorders on oak in Europe. *Forestry* **2014**, *87*, 535–551. [CrossRef]
11. Denman, S.; Webber, J. Oak declines: New definitions and new episodes in Britain. *Q. J. For.* **2009**, *103*, 285–290.
12. Brady, C.; Arnold, D.; McDonald, J.; Denman, S. Taxonomy and identification of bacteria associated with acute oak decline. *World J. Microbiol. Biotechnol.* **2017**, *33*, 143. [CrossRef]
13. Denman, S.; Plummer, S.; Kirk, S.; Peace, A.; McDonald, J.E. Isolation studies reveal a shift in the cultivable microbiome of oak affected with Acute Oak Decline. *Syst. Appl. Microbiol.* **2016**, *39*, 484–490. [CrossRef]
14. Denman, S.; Doonan, J.; Ransom-Jones, E.; Broberg, M.; Plummer, S.; Kirk, S.; Scarlett, K.; Griffiths, A.R.; Kaczmarek, M.; Forster, J.; et al. Microbiome and infectivity studies reveal complex polyspecies tree disease in Acute Oak Decline. *ISME J.* **2018**, *12*, 386–399. [CrossRef] [PubMed]
15. Doonan, J.; Denman, S.; Pachebat, J.A.; McDonald, J.E. Genomic analysis of bacteria in the Acute Oak Decline pathobiome. *Microb. Genom.* **2019**, *5*. [CrossRef]
16. Hacquard, S.; Schadt, C.W. Towards a holistic understanding of the beneficial interactions across the *Populus* microbiome. *New Phytol.* **2015**, *205*, 1424–1430. [CrossRef]
17. Vandenkoornhuyse, P.; Quaiser, A.; Duhamel, M.; Le Van, A.; Dufresne, A. The importance of the microbiome of the plant holobiont. *New Phytol.* **2015**, *206*, 1196–1206. [CrossRef] [PubMed]
18. Berendsen, R.L.; Pieterse, C.M.J.; Bakker, P.A.H.M. The rhizosphere microbiome and plant health. *Trends Plant Sci.* **2012**, *17*, 478–486. [CrossRef] [PubMed]
19. Buée, M.; De Boer, W.; Martin, F.; van Overbeek, L.; Jurkevitch, E. The rhizosphere zoo: An overview of plant-associated communities of microorganisms, including phages, bacteria, archaea, and fungi, and of some of their structuring factors. *Plant Soil* **2009**, *321*, 189–212. [CrossRef]
20. Uroz, S.; Oger, P.; Tisserand, E.; Cébron, A.; Turpault, M.-P.; Buée, M.; De Boer, W.; Leveau, J.H.J.; Frey-Klett, P. Specific impacts of beech and Norway spruce on the structure and diversity of the rhizosphere and soil microbial communities. *Sci. Rep.* **2016**, *6*, 27756. [CrossRef]
21. Uroz, S.; Buée, M.; Murat, C.; Frey-Klett, P.; Martin, F. Pyrosequencing reveals a contrasted bacterial diversity between oak rhizosphere and surrounding soil. *Environ. Microbiol. Rep.* **2010**, *2*, 281–288. [CrossRef]

22. Sasse, J.; Martinoia, E.; Northen, T. Feed Your Friends: Do Plant Exudates Shape the Root Microbiome? *Trends Plant Sci.* **2018**, *23*, 25–41. [CrossRef]
23. Gottel, N.R.; Castro, H.F.; Kerley, M.; Yang, Z.; Pelletier, D.A.; Podar, M.; Karpinets, T.; Uberbacher, E.; Tuskan, G.A.; Vilgalys, R.; et al. Distinct microbial communities within the endosphere and rhizosphere of Populus deltoides roots across contrasting soil types. *Appl. Environ. Microbiol.* **2011**, *77*, 5934–5944. [CrossRef]
24. Beckers, B.; Op De Beeck, M.; Weyens, N.; Boerjan, W.; Vangronsveld, J. Structural variability and niche differentiation in the rhizosphere and endosphere bacterial microbiome of field-grown poplar trees. *Microbiome* **2017**, *5*, 25. [CrossRef] [PubMed]
25. Cobo-Díaz, J.; Fernández-González, A.; Villadas, P.; Toro, N.; Tringe, S.; Fernández-López, M.; Cobo-Díaz, J.F.; Fernández-González, A.J.; Villadas, P.J.; Toro, N.; et al. Taxonomic and Functional Diversity of a Quercus pyrenaica Willd. Rhizospheric Microbiome in the Mediterranean Mountains. *Forests* **2017**, *8*, 390. [CrossRef]
26. Gallart, M.; Adair, K.L.; Love, J.; Meason, D.F.; Clinton, P.W.; Xue, J.; Turnbull, M.H. Host Genotype and Nitrogen Form Shape the Root Microbiome of Pinus radiata. *Microb. Ecol.* **2018**, *75*, 419–433. [CrossRef]
27. Seaton, F.M.; Barrett, G.; Burden, A.; Creer, S.; Fitos, E.; Garbutt, A.; Griffiths, R.I.; Henrys, P.; Jones, D.L.; Keenan, P.; et al. Soil health cluster analysis based on national monitoring of soil indicators. *Eur. J. Soil Sci.* **2020**. [CrossRef]
28. Bünemann, E.K.; Bongiorno, G.; Bai, Z.; Creamer, R.E.; De Deyn, G.; de Goede, R.; Fleskens, L.; Geissen, V.; Kuyper, T.W.; Mäder, P.; et al. Soil quality—A critical review. *Soil Biol. Biochem.* **2018**, *120*, 105–125. [CrossRef]
29. Gärdenäs, A.I.; Ågren, G.I.; Bird, J.A.; Clarholm, M.; Hallin, S.; Ineson, P.; Kätterer, T.; Knicker, H.; Nilsson, S.I.; Näsholm, T.; et al. Knowledge gaps in soil carbon and nitrogen interactions—From molecular to global scale. *Soil Biol. Biochem.* **2011**, *43*, 702–717. [CrossRef]
30. Brown, N.; Jeger, M.; Kirk, S.; Xu, X.; Denman, S. Spatial and temporal patterns in symptom expression within eight woodlands affected by Acute Oak Decline. *For. Ecol. Manag.* **2016**, *360*, 97–109. [CrossRef]
31. Gibbs, J.; Greig, B.J.W. Biotic and abiotic factors affecting the dying back of pedunculate oak *Quercus robur* L. *Forestry* **1997**, *70*, 399–406. [CrossRef]
32. Herlemann, D.P.; Labrenz, M.; Jürgens, K.; Bertilsson, S.; Waniek, J.J.; Andersson, A.F. Transitions in bacterial communities along the 2000 km salinity gradient of the Baltic Sea. *ISME J.* **2011**, *5*, 1571–1579. [CrossRef]
33. Klindworth, A.; Pruesse, E.; Schweer, T.; Peplies, J.; Quast, C.; Horn, M.; Glöckner, F.O. Evaluation of general 16S ribosomal RNA gene PCR primers for classical and next-generation sequencing-based diversity studies. *Nucleic Acids Res.* **2013**, *41*. [CrossRef]
34. Tedersoo, L.; Bahram, M.; Polme, S.; Koljalg, U.; Yorou, N.S.; Wijesundera, R.; Ruiz, L.V.; Vasco-Palacios, A.M.; Thu, P.Q.; Suija, A.; et al. Global diversity and geography of soil fungi. *Science* **2014**, *346*, 1256688. [CrossRef]
35. Illumina 16S Metagenomic Sequencing Library Preparation. Available online: https://support.illumina.com/content/dam/illumina-support/documents/documentation/chemistry_documentation/16s/16s-metagenomic-library-prep-guide-15044223-b.pdf (accessed on 25 October 2020).
36. Schmieder, R.; Edwards, R. Quality control and preprocessing of metagenomic datasets. *Bioinformatics* **2011**, *27*, 863–864. [CrossRef] [PubMed]
37. Schubert, M.; Lindgreen, S.; Orlando, L. AdapterRemoval v2: Rapid adapter trimming, identification, and read merging. *BMC Res. Notes* **2016**, *9*, 88. [CrossRef]
38. Edgar, R.C. Search and clustering orders of magnitude faster than BLAST. *Bioinformatics* **2010**, *26*, 2460–2461. [CrossRef]
39. Bengtsson-Palme, J.; Ryberg, M.; Hartmann, M.; Branco, S.; Wang, Z.; Godhe, A.; De Wit, P.; Sánchez-García, M.; Ebersberger, I.; de Sousa, F.; et al. Improved software detection and extraction of ITS1 and ITS2 from ribosomal ITS sequences of fungi and other eukaryotes for analysis of environmental sequencing data. *Methods Ecol. Evol.* **2013**, *4*, 914–919. [CrossRef]
40. Caporaso, J.G.; Kuczynski, J.; Stombaugh, J.; Bittinger, K.; Bushman, F.D.; Costello, E.K.; Fierer, N.; Peña, A.G.; Goodrich, J.K.; Gordon, J.I.; et al. QIIME allows analysis of high-throughput community sequencing data. *Nat. Methods* **2010**, *7*, 335–336. [CrossRef] [PubMed]
41. DeSantis, T.Z.; Hugenholtz, P.; Larsen, N.; Rojas, M.; Brodie, E.L.; Keller, K.; Huber, T.; Dalevi, D.; Hu, P.; Andersen, G.L. Greengenes, a chimera-checked 16S rRNA gene database and workbench compatible with ARB. *Appl. Environ. Microbiol.* **2006**, *72*, 5069–5072. [CrossRef]

42. Kõljalg, U.; Nilsson, R.H.; Abarenkov, K.; Tedersoo, L.; Taylor, A.F.S.; Bahram, M.; Bates, S.T.; Bruns, T.D.; Bengtsson-Palme, J.; Callaghan, T.M.; et al. Towards a unified paradigm for sequence-based identification of fungi. *Mol. Ecol.* **2013**, *22*, 5271–5277. [CrossRef]
43. Clarke, K.; Gorley, R. *PRIMER v6: User Manual/Tutorial*; PRIMER-E: Plymouth, UK, 2006.
44. Clarke, K.R.; Ainsworth, M. A method of linking multivariate community structure to environmental variables. *Mar. Ecol. Prog. Ser.* **1993**, *92*, 205–219. [CrossRef]
45. Nguyen, N.H.; Song, Z.; Bates, S.T.; Branco, S.; Tedersoo, L.; Menke, J.; Schilling, J.S.; Kennedy, P.G. FUNGuild: An open annotation tool for parsing fungal community datasets by ecological guild. *Fungal Ecol.* **2016**, *20*, 241–248. [CrossRef]
46. Love, M.I.; Huber, W.; Anders, S. Moderated estimation of fold change and dispersion for RNA-seq data with DESeq2. *Genome Biol.* **2014**, *15*, 550. [CrossRef] [PubMed]
47. Dhariwal, A.; Chong, J.; Habib, S.; King, I.L.; Agellon, L.B.; Xia, J. MicrobiomeAnalyst: A web-based tool for comprehensive statistical, visual and meta-analysis of microbiome data. *Nucleic Acids Res.* **2017**, *45*, W180–W188. [CrossRef] [PubMed]
48. Mauri, M.; Elli, T.; Caviglia, G.; Uboldi, G.; Azzi, M. RAWGraphs. In Proceedings of the 12th Biannual Conference on Italian SIGCHI Chapter—CHItaly '17, Cagliari, Italy, 18–20 September 2017; ACM Press: New York, NY, USA, 2017; pp. 1–5.
49. IBM Corp. *IBM SPSS Statistics for Windows, Version 22.0*; IBM Corp.: Armonk, NY, USA, 2013.
50. Spatafora, J.W.; Chang, Y.; Benny, G.L.; Lazarus, K.; Smith, M.E.; Berbee, M.L.; Bonito, G.; Corradi, N.; Grigoriev, I.; Gryganskyi, A.; et al. A phylum-level phylogenetic classification of zygomycete fungi based on genome-scale data. *Mycologia* **2016**, *108*, 1028–1046. [CrossRef]
51. Grayston, S.J.; Vaughan, D.; Jones, D. Rhizosphere carbon flow in trees, in comparison with annual plants: The importance of root exudation and its impact on microbial activity and nutrient availability. *Appl. Soil Ecol.* **1997**, *5*, 29–56. [CrossRef]
52. Karst, J.; Gaster, J.; Wiley, E.; Landhäusser, S.M. Stress differentially causes roots of tree seedlings to exude carbon. *Tree Physiol.* **2016**, *37*, 154–164. [CrossRef] [PubMed]
53. Gargallo-Garriga, A.; Preece, C.; Sardans, J.; Oravec, M.; Urban, O.; Peñuelas, J. Root exudate metabolomes change under drought and show limited capacity for recovery. *Sci. Rep.* **2018**, *8*, 12696. [CrossRef] [PubMed]
54. Hinsinger, P.; Plassard, C.; Tang, C.; Jaillard, B. Origins of root-mediated pH changes in the rhizosphere and their responses to environmental constraints: A review. *Plant Soil* **2003**, *248*, 43–59. [CrossRef]
55. Cregger, M.A.; Veach, A.M.; Yang, Z.K.; Crouch, M.J.; Vilgalys, R.; Tuskan, G.A.; Schadt, C.W. The Populus holobiont: Dissecting the effects of plant niches and genotype on the microbiome. *Microbiome* **2018**, *6*, 31. [CrossRef]
56. Paterson, E.; Gebbing, T.; Abel, C.; Sim, A.; Telfer, G. Rhizodeposition shapes rhizosphere microbial community structure in organic soil. *New Phytol.* **2007**, *173*, 600–610. [CrossRef]
57. Badri, D.; Vivanco, J. Regulation and function of root exudates. *Plant. Cell Environ.* **2009**, *32*, 666–681. [CrossRef]
58. Timm, C.M.; Carter, K.R.; Carrell, A.A.; Jun, S.-R.; Jawdy, S.S.; Vélez, J.M.; Gunter, L.E.; Yang, Z.; Nookaew, I.; Engle, N.L.; et al. Abiotic Stresses Shift Belowground Populus-Associated Bacteria Toward a Core Stress Microbiome. *mSystems* **2018**, *3*. [CrossRef] [PubMed]
59. Fierer, N. Embracing the unknown: Disentangling the complexities of the soil microbiome. *Nat. Rev. Microbiol.* **2017**, *15*, 579–590. [CrossRef] [PubMed]
60. Lee, S.-H.; Ka, J.-O.; Cho, J.-C. Members of the phylum *Acidobacteria* are dominant and metabolically active in rhizosphere soil. *FEMS Microbiol. Lett.* **2008**, *285*, 263–269. [CrossRef]
61. Ward, N.L.; Challacombe, J.F.; Janssen, P.H.; Henrissat, B.; Coutinho, P.M.; Wu, M.; Xie, G.; Haft, D.H.; Sait, M.; Badger, J.; et al. Three genomes from the phylum Acidobacteria provide insight into the lifestyles of these microorganisms in soils. *Appl. Environ. Microbiol.* **2009**, *75*, 2046–2056. [CrossRef] [PubMed]
62. Eichorst, S.A.; Trojan, D.; Roux, S.; Herbold, C.; Rattei, T.; Woebken, D. Genomic insights into the *Acidobacteria* reveal strategies for their success in terrestrial environments. *Environ. Microbiol.* **2018**, *20*, 1041–1063. [CrossRef] [PubMed]
63. Kielak, A.M.; Cipriano, M.A.P.; Kuramae, E.E. Acidobacteria strains from subdivision 1 act as plant growth-promoting bacteria. *Arch. Microbiol.* **2016**, *198*, 987–993. [CrossRef]

64. Van Kessel, M.A.H.J.; Speth, D.R.; Albertsen, M.; Nielsen, P.H.; Op Den Camp, H.J.M.; Kartal, B.; Jetten, M.S.M.; Lücker, S. Complete nitrification by a single microorganism. *Nature* **2015**, *528*, 555–559. [CrossRef]
65. Smith, S.E.; Read, D.J.; David, J. *Mycorrhizal Symbiosis*; Academic Press: London, UK, 2008; ISBN 9780123705266.
66. Bonfante, P.; Genre, A. Mechanisms underlying beneficial plant–fungus interactions in mycorrhizal symbiosis. *Nat. Commun.* **2010**, *1*, 1–11. [CrossRef]
67. Suz, L.M.; Barsoum, N.; Benham, S.; Dietrich, H.-P.; Fetzer, K.D.; Fischer, R.; García, P.; Gehrman, J.; Kristöfel, F.; Manninger, M.; et al. Environmental drivers of ectomycorrhizal communities in Europe's temperate oak forests. *Mol. Ecol.* **2014**, *23*, 5628–5644. [CrossRef]
68. van der Linde, S.; Suz, L.M.; Orme, C.D.L.; Cox, F.; Andreae, H.; Asi, E.; Atkinson, B.; Benham, S.; Carroll, C.; Cools, N.; et al. Environment and host as large-scale controls of ectomycorrhizal fungi. *Nature* **2018**, *558*, 243–248. [CrossRef]
69. Avis, P.G.; Mueller, G.M.; Lussenhop, J. Ectomycorrhizal fungal communities in two North American oak forests respond to nitrogen addition. *New Phytol.* **2008**, *179*, 472–483. [CrossRef]
70. Avis, P.G.; McLaughlin, D.J.; Dentinger, B.C.; Reich, P.B. Long-term increase in nitrogen supply alters above- and below-ground ectomycorrhizal communities and increases the dominance of Russula spp. in a temperate oak savanna. *New Phytol.* **2003**, *160*, 239–253. [CrossRef]
71. Cox, F.; Barsoum, N.; Lilleskov, E.A.; Bidartondo, M.I. Nitrogen availability is a primary determinant of conifer mycorrhizas across complex environmental gradients. *Ecol. Lett.* **2010**, *13*, 1103–1113. [CrossRef]
72. Lilleskov, E.A.; Hobbie, E.A.; Horton, T.R. Conservation of ectomycorrhizal fungi: Exploring the linkages between functional and taxonomic responses to anthropogenic N deposition. *Fungal Ecol.* **2011**, *4*, 174–183. [CrossRef]
73. Chapelle, E.; Mendes, R.; Bakker, P.A.H.; Raaijmakers, J.M. Fungal invasion of the rhizosphere microbiome. *ISME J.* **2016**, *10*, 265–268. [CrossRef] [PubMed]
74. Gordon, T.R.; Kirkpatrick, S.C.; Aegerter, B.J.; Wood, D.L.; Storer, A.J. Susceptibility of Douglas fir (*Pseudotsuga menziesii*) to pitch canker, caused by Gibberella circinata (anamorph = *Fusarium circinatum*). *Plant Pathol.* **2006**, *55*, 231–237. [CrossRef]
75. Aegerter, B.J.; Gordon, T.R. Rates of pitch canker induced seedling mortality among Pinus radiata families varying in levels of genetic resistance to Gibberella circinata (anamorph *Fusarium circinatum*). *For. Ecol. Manag.* **2006**, *235*, 14–17. [CrossRef]
76. Gramaje, D.; Mostert, L.; Groenewald, J.Z.; Crous, P.W. Phaeoacremonium: From esca disease to phaeohyphomycosis. *Fungal Biol.* **2015**, *119*, 759–783. [CrossRef]
77. Hartmann, M.; Niklaus, P.A.; Zimmermann, S.; Schmutz, S.; Kremer, J.; Abarenkov, K.; Lüscher, P.; Widmer, F.; Frey, B. Resistance and resilience of the forest soil microbiome to logging-associated compaction. *ISME J.* **2014**, *8*, 226–244. [CrossRef]
78. Šťursová, M.; Šnajdr, J.; Cajthaml, T.; Bárta, J.; Šantrůčková, H.; Baldrian, P. When the forest dies: The response of forest soil fungi to a bark beetle-induced tree dieback. *ISME J.* **2014**, *8*, 1920–1931. [CrossRef]